Electrically tunable charge and spin transitions in Landau levels of interacting Dirac fermions in trilayer graphene

Vadim M. Apalkov
Department of Physics and Astronomy, Georgia State University, Atlanta, Georgia 30303, USA

Tapash Chakraborty*
Department of Physics and Astronomy, University of Manitoba, Winnipeg, Canada R3T 2N2

(Received 14 November 2011; published 5 July 2012)

Trilayer graphene in the fractional quantum Hall effect regime displays a set of unique interaction-induced transitions that can be tuned entirely by the applied bias voltage. These transitions occur near the anticrossing points of two Landau levels. In a large magnetic field (>8 T) the electron-electron interactions close the anticrossing gap, resulting in some unusual transitions between different Landau levels. For the filling factor $\nu = \frac{2}{3}$, these transitions are accompanied by a change of spin polarization of the ground state. For small Zeeman energy, this provides a unique opportunity to control the spin polarization of the ground state by fine tuning the bias voltage.

DOI: 10.1103/PhysRevB.86.035401 PACS number(s): 73.43.Cd, 73.21.Ac, 73.50.Bk, 73.61.Wp

I. INTRODUCTION

Dirac fermions in monolayer and bilayer graphene with their remarkable electronic properties have received extraordinary scrutiny in recent years.[1,2] In an external magnetic field these systems exhibit unconventional quantum Hall effects[3,4] that are direct manifestations of their rather unusual band structures.[5,6] As a consequence, the Landau level (LL) energies of these systems are very different from those of conventional two-dimensional electron systems. In monolayer graphene the Landau level energies exhibit a square root dependence on the applied field,[7] while a linear dependence is observed in bilayer graphene.[8] Interactions among Dirac fermions in the fractional quantum Hall effect (FQHE)[9,10] regime reveal several unexpected and intriguing effects in monolayer[11] and bilayer[12] graphene. Experimental observation of FQHE in monolayer graphene[13,14] has indeed confirmed the important role electron-electron interactions play in these systems. Clearly, the dynamics of Dirac fermions are sensitive to the number of graphene layers present in the system and their stacking arrangements. The attention has naturally shifted to the investigation of the electronic properties of Dirac fermions in trilayer graphene (TLG).

A TLG consisting of three coupled graphene layers (see Fig. 1) has a very unique electronic energy spectrum. Within the nearest-neighbor interlayer coupling approximation the energy spectrum of TLG with Bernal stacking consists effectively of decoupled single-layer graphene and the bilayer graphene energy spectra. Therefore it allows us to study the energy spectra of both the massless and massive Dirac fermions within a single system. In a strong perpendicular magnetic field, the LL energy spectrum of TLG becomes a combination of Landau levels of single-layer and bilayer graphene.[15] The spectrum exhibits many crossings of the LLs as a function of the magnetic field. At the crossing points the LLs are highly degenerate. The degeneracy is lifted when higher-order interlayer coupling terms are taken into account, resulting in several unusual properties of the quantum Hall effect (QHE) in trilayer graphene.[16]

While the single-particle features of the QHE are interesting, here we report that interactions among Dirac fermions in a TLG in the FQHE regime result in very unique properties of the TLG that are far beyond the mere level crossings observed in the integer QHE. We found several LL repulsions and level crossings which resulted in some intriguing spin transitions among the LLs in this system that have no analogues in the interaction-induced spin-reversed ground states and elementary excitations discovered earlier in conventional electron systems.[17,18] These spin transitions in the TLG are driven by an applied perpendicular bias field for a fixed magnetic field, and therefore we expect these novel transitions to be entirely tunable. These transitions are not expected in a bilayer graphene. The origin of these many-body transitions in TLG lies in the higher-order couplings, γ_2 and γ_5, between layers 1 and 3 [Fig. 1] that are responsible for the anticrossings, the gap of which is comparable to the FQHE energy gap.

II. THEORETICAL APPROACH

We only consider the Bernal or ABA-stacking of our TLG (Fig. 1). In the tight-binding approximation the Hamiltonian of the TLG is characterized by the intralayer hopping integral, $\gamma_0 = 3.1$ eV, and interlayer hopping integrals, $\gamma_1 = 0.39$ eV, $\gamma_2 = -0.028$ eV, $\gamma_4 = 0.041$ eV, and $\gamma_5 = 0.05$ eV, corresponding to different types of interlayer coupling, shown schematically in Fig. 1.[16] In the basis $(\psi_{A_1} - \psi_{A_3}, \psi_{B_1} - \psi_{B_3}, \psi_{A_1} + \psi_{A_3}, \psi_{B_2}, \psi_{A_2}, \psi_{B_1} + \psi_{B_3})$ and in a perpendicular magnetic field, the Hamiltonian of a TLG for a single valley, e.g.,

valley K, takes the form[15,16]

$$\mathcal{H} = \begin{pmatrix} -\gamma_2/2 & v_0\pi_+ & -U/2 & 0 & 0 & 0 \\ v_0\pi_- & -\gamma_5/2+\delta & 0 & 0 & 0 & -U/2 \\ -U/2 & 0 & +\gamma_2/2 & 0 & -\sqrt{2}v_4\pi_+ & v_0\pi_+ \\ 0 & 0 & 0 & 0 & v_0\pi_- & -\sqrt{2}v_4\pi_- \\ 0 & 0 & -\sqrt{2}v_4\pi_- & v_0\pi_+ & \delta & \sqrt{2}\gamma_1 \\ 0 & -U/2 & v_0\pi_- & -\sqrt{2}v_4\pi_+ & \sqrt{2}\gamma_1 & \gamma_5/2+\delta \end{pmatrix}, \quad (1)$$

where $v_0 = (\sqrt{3}/2)a\gamma_0/\hbar \approx 10^6$ m/s, $v_4 = (\sqrt{3}/2)a\gamma_4/\hbar$, and $\pi_\pm = \pi_x \pm \pi_y$. Here $\vec{\pi} = \vec{p} + e\vec{A}/c$ is the generalized momentum. The parameter $\delta = 0.046$ eV is the difference between the on-site energies of two sublattices within a single graphene layer.[16] The bias voltage U, which is externally varied, is the potential difference, i.e., the on-site energy difference between layers 1 and 3. The potentials of layers 1–3 are assumed to be 0, $U/2$, and U, respectively. The interlayer couplings γ_2 and γ_5 and the finite bias voltage U break the valley symmetry of the trilayer Hamiltonian and lift the valley degeneracy of the TLG system. Without the Zeeman energy each level has a two-fold spin degeneracy.

The LLs of a TLG are obtained from the Hamiltonian (1). The corresponding wave functions are parametrized by the integer $n \geqslant -2$ and are expressed in terms of the conventional (*nonrelativistic*) Landau level functions, $\phi_{n,m}$

$$\Psi = \begin{pmatrix} C_1\phi_{n+2,m} \\ C_2\phi_{n+1,m} \\ C_3\phi_{n+2,m} \\ C_4\phi_{n,m} \\ C_5\phi_{n+1,m} \\ C_6\phi_{n+1,m} \end{pmatrix},$$

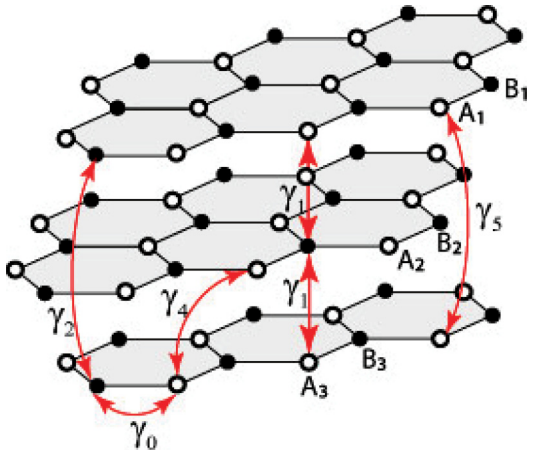

FIG. 1. (Color online) TLG in ABA stacking (schematic). Each layer consists of two inequivalent sites A and B. The interlayer and intralayer hopping integrals, γ_i, show the couplings which are included in the single-particle Hamiltonian (1).

for $n \geqslant 0$;

$$\Psi = \begin{pmatrix} C_1\phi_{1,m} \\ C_2\phi_{0,m} \\ C_3\phi_{1,m} \\ 0 \\ C_5\phi_{0,m} \\ C_6\phi_{0,m} \end{pmatrix},$$

for $n = -1$, and

$$\Psi = \begin{pmatrix} C_1\phi_{0,m} \\ 0 \\ C_3\phi_{0,m} \\ 0 \\ 0 \\ 0 \end{pmatrix},$$

for $n = -2$. Here m is the intra-Landau level parameter, e.g., the angular momentum, and C_i are constants. Therefore, the LL wave functions of a TLG are combinations of $n, n+1$, and $n+2$ nonrelativistic Landau functions.

We consider a many-electron system with partial occupation of a single LL of the TLG. We have studied the properties of these systems in the FQHE regime, specifically for filling factors, $\nu = \frac{1}{3}, \frac{2}{3}$, and $\frac{2}{5}$. In these cases, the conventional nonrelativistic system shows incompressible behavior with a finite energy gap.[9,10] The interaction properties of the many-electron system occupying a single Landau level are completely determined by the Haldane pseudopotentials $V_m^{(n)}$,[19] which are the interaction energies of two electrons with relative angular momentum m. These pseudopotentials are evaluated from the following expression:[19]

$$V_m^{(n)} = \int_0^\infty \frac{dq}{2\pi} q V(q) [F_n(q)]^2 L_m(q^2) e^{-q^2}, \quad (2)$$

where $L_m(x)$ are the Laguerre polinomials, $V(q) = 2\pi e^2/(\kappa \ell_0 q)$ is the Coulomb interaction in the momentum space, κ is the dielectric constant, $\ell_0 = \sqrt{e\hbar/cB}$ is the magnetic length, and $F_n(q)$ is the form factor of the nth Landau level ($n \geqslant -2$). The form factor is completely determined by the LL wave functions. With the known wave functions, the form factors for the corresponding Landau level of TLG can be evaluated from

$$\begin{aligned} F_{n\geqslant 0}(q) = {} & [|C_2|^2 + |C_5|^2 + |C_6|^2] L_{n+1}(q^2/2) \\ & + [|C_1|^2 + |C_3|^2] L_{n+2}(q^2/2) \\ & + |C_4|^2 L_n(q^2/2), \end{aligned} \quad (3)$$

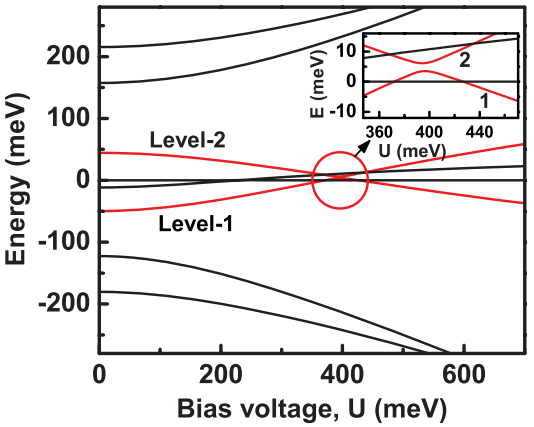

FIG. 2. (Color online) LL spectrum of TLG in 15 T magnetic field as a function of the bias voltage, U. Two red lines show anticrossing for $U \approx 400$ meV. The corresponding LLs are labeled as level-1 and level-2, respectively. The LLs 1 and 2 belong to the set of Landau levels with parameter $n = 0$. The inset shows the region of anticrossing. The anticrossing gap is ≈2.6 meV ≈ 30 K.

$$F_{n=-1}(q) = [|C_2|^2 + |C_5|^2 + |C_6|^2]L_0(q^2/2) + [|C_1|^2 + |C_3|^2]L_1(q^2/2), \quad (4)$$

and

$$F_{n=-2}(q) = [|C_1|^2 + |C_3|^2]L_0(q^2/2). \quad (5)$$

We study the FQHE state in a TLG by considering a finite-size system of N electrons in a spherical geometry[19] with interaction potentials determined by the Haldane pseudopotentials. The radius of the sphere is $\sqrt{S}\ell_0$, where $2S$ is the number of magnetic fluxes through the sphere in units of the flux quantum. The parameter S also determines the number of single-particles states, $2S + 1$, and for a finite number of electrons–the filling factor of the system.[20] For example, the filling factor $\nu = \frac{1}{p}$ is realized for $2S = p(N - 1)$.

III. RESULTS AND DISCUSSION

From the Hamiltonian (1) we evaluate the single-particle LL energy spectrum. The LLs are parametrized by the integer n [see Eq. (2)]; for each n there are 6 LLs. A typical LL spectrum is shown in Fig. 2. The spectrum as a function of U (or the magnetic field) shows crossing and anticrossing of the energy levels. The anticrossing gap (ACG) in Fig. 2 is about 2.6 meV ≈30 K for a field of 15 T. Near these anticrossing points (ACPs) the FQHE has nontrivial and unique interaction-induced properties. We focus our attention near the special ACP shown as the inset in Fig. 2. This point corresponds to anticrossing of the LLs with $n = 0$. We label the corresponding levels as Landau level-1 (LL-1) and Landau level-2 (LL-2) [Fig. 2] and consider the FQHE states only in these levels. For each FQHE state we have evaluated the ground state energy per particle and the FQHE excitation gap.

We first consider the fundamental $\nu = \frac{1}{3}$-FQHE states in LLs 1 and 2 (Fig. 3). The system behaves very differently for weak and strong magnetic fields. In a weak magnetic field ($B = 5$ T) the many-particle states show an anticrossing [Fig. 1], just as for the single-particle levels [Fig. 2]. This

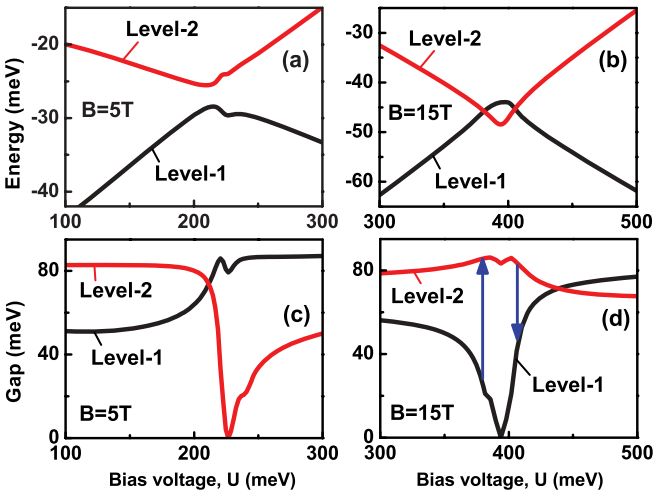

FIG. 3. (Color online) Results for $\nu = \frac{1}{3}$-FQHE states in LL 1 and LL 2, shown as a function of the bias voltage near the anticrossing point. Panels (a) and (b) show the ground state energy per particle, while panels (c) and (d) show the excitation gaps for the corresponding energy levels with filling factor $\nu = \frac{1}{3}$. Blue arrows in panel (d) indicate jumps of the FQHE gaps at the level crossing in panel (b). The number of electrons is $N = 9$ and the parameter of the sphere is $2S = 24$.

anticrossing is clearly visible in the dependence of the $\frac{1}{3}$-FQHE gaps since the values of the FQHE gaps in LL-1 and LL-2 are interchanged when the system goes through the ACP. The system shows an interesting behavior exactly at the ACP. Here, due to a mixture of the single-particle wave functions of LL-1 and LL-2, the many-particle interaction properties are enhanced in LL-1 while suppressed in LL-2. As a result, at the ACP the $\frac{1}{3}$-FQHE gap in LL-1 has a maximum while the $\frac{1}{3}$-state in LL-2 becomes compressible with a vanishing gap [Fig. 3(c)]. Due to a larger cohesive energy of the incompressible state compared to the compressible one, the many-particle ACG shows a small enhancement relative to the single-particle value by 0.4 meV ≈ 5 K. Experimentally, the anticrossing properties of TLG in a small magnetic field can be observed by studying the FQHE in LL-2. In such a system, with increasing bias voltage one would observe a transition FQHE–no FQHE–FQHE within a single LL, just as we predicted earlier for bilayer graphene.[12]

In a large magnetic field ($B = 15$ T), TLG shows several novel features near the ACP [Figs. 3(b) and 3(d)]: The anticrossing of the single-particle energy levels becomes double crossings for the many-particle states. This means that the cohesive energy of the many-particle state in LL-2 is larger than that in LL-1, and this difference overcomes the ACG. The reason for such a behavior is the change in the interaction strength in LL-1 and LL-2.

For a large magnetic field the many-particle interaction potential at the ACP becomes *stronger* in LL-2 and *weaker* in LL-1, which is opposite to what we see for a weak magnetic field [Figs. 3(a) and 3(c)]. As a result, the FQHE gap in LL-2 has a maximum at the ACP, while the gap in LL-1 is suppressed. Therefore at the ACP the $\nu = \frac{1}{3}$-many-particle system is incompressible in LL-2 and compressible in LL-1. Since the incompressible FQHE state has a lower

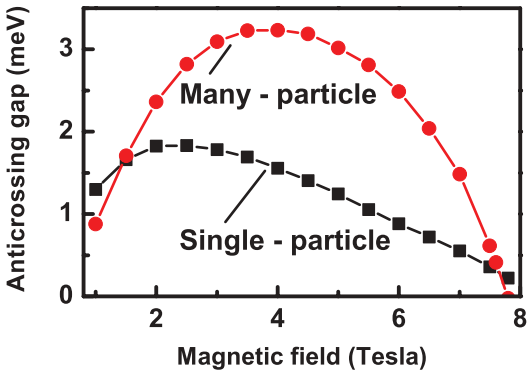

FIG. 4. (Color online) The ACG corresponding to the anticrossing of LL-1 and LL-2 [Fig. 1(b)], versus the magnetic field. For different magnetic fields, anticrossings occur for different bias voltages. The black line and the squares describe a single-particle system, while the red line and the circles correspond to the many-particle $\nu = \frac{1}{3}$-FQHE state (Fig. 2). The single-particle ACG is closed for the many-particle system for $B \sim 8$ T.

binding energy than that of the compressible state, this energy difference is enough to close the ACG. Therefore, in a large magnetic field and as a function of the bias voltage, we should expect the following behavior: The FQHE state, which initially for $U < 400$ meV, is in LL-1, occupies LL-2 at the ACP, $U = 400$ meV, leaving LL-1 empty. For $U > 400$ meV, the system returns to LL-1, while LL-2 becomes empty. These transitions between different LLs at the ACP are accompanied by jumps in the value of the FQHE gap [blue lines in Fig. 3(d)].

The strength of FQHE, i.e., the magnitude of the FQHE gap, and correspondingly the cohesive energy of the FQHE states, is determined by the short-range properties of the interaction potential, i.e, the Haldane pseudopotentials for small values of the relative angular momentum, m. There, at the ACP the short-range interaction strength is enhanced in LL-1 for weak magnetic fields and in LL-2 for high magnetic fields. This results in a weak enhancement of the many-particle ACG for weak magnetic fields and strong suppression of the many-particle ACG for strong magnetic fields. In Fig. 4, the ACGs for single-particle and many-particle $\nu = \frac{1}{3}$-FQHE state are shown for different magnetic fields. For small values of the magnetic fields, $1.5\ \text{T} < B < 8\ \text{T}$, the many-particle gap clearly shows an enhancement compared to that for the single-particle case. The many-particle and single-particle ACGs show almost parabolic dependence on the magnetic field, where the many-particle gap shows stronger dependence with a width that is about one-fifth of that of the single-particle gap. For $B \approx 8$ T the many-particle ACG closes, and for $B > 8$ T the anticrossing in a single-particle system becomes a double-crossing in the many-particle FQHE state.

The FQHE ground state of conventional semiconductor systems is known to be either spin-polarized or spin-unpolarized. The polarization properties of the system are determined by the filling factor and strength of the applied magnetic field.[10,17] While in conventional systems the $\nu = \frac{1}{m}$ FQHE state is always fully spin-polarized, for filling factors $\nu = \frac{2}{3}$ and $\nu = \frac{2}{5}$ there is a competition between the energies of spin-polarized and spin-unpolarized incompressible states.[17] With increasing strength of the magnetic field, the Zeeman energy of electrons favors the spin-polarized state, which results in possible spin transitions in the system by varying the magnetic field. Those theoretical predictions subsequently received experimental confirmation.[18,21] In fact, TLG shows a *different type of spin transitions* realized at the ACPs, which could also be probed experimentally. Spin transitions in the FQHE regime for a conventional semiconductor system are determined by the competition between the Zeeman energy and the difference between the cohesive energies of the spin-polarized and spin-unpolarized ground states. Therefore, the spin transitions in conventional systems are driven by the Zeeman energy. In the present system the spin transitions are determined by a modification of the interaction potentials in a given Landau level. This modification is due to the anticrossing of the energy levels, which influences the single-particle wave functions and correspondingly changes the interelectron interaction strength. Therefore in this case, by changing the parameters of the system (e.g., the bias voltage) we change the interelectron interaction, and spin transitions at $2/3$ filling factor should be possible even for zero Zeeman energy.

The spin properties of the FQHE states in TLG are analyzed for filling factors $\nu = \frac{2}{3}$ and $\nu = \frac{2}{5}$. In Fig. 5 the results for the $\nu = \frac{2}{3}$-FQHE state are shown for LL-1 and LL-2 without including the Zeeman energy. The black and red lines in Figs. 5(a) and 5(b) correspond to spin-polarized and spin-unpolarized states, respectively. The general behavior of the state is similar to that of the $\nu = \frac{1}{3}$ state. For small magnetic fields there are stronger interactions in LL-1, while for larger magnetic fields the anticrossing of energy levels becomes double crossings. For a small magnetic field, the ground state of the $\nu = \frac{2}{3}$ state is mainly spin-polarized with only a small region of bias voltages, U, when the system becomes spin-unpolarized in LL-2. Therefore, for a weak magnetic

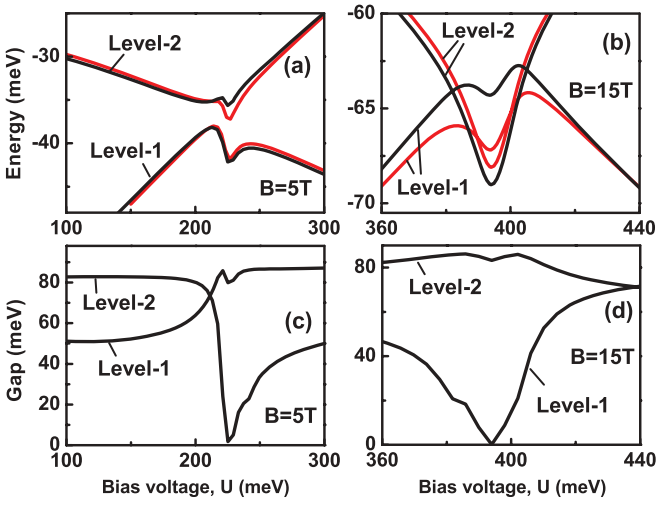

FIG. 5. (Color online) The ground state energy per particle [panels (a) and (b)] and the excitation gaps [panels (c) and (d)] for $\nu = \frac{2}{3}$ in LL-1 and LL-2 versus the bias voltage near the ACPs. The excitation gaps are shown only for the spin-polarized systems. The black and red lines in panels (a) and (b) correspond to spin-polarized and spin-unpolarized states, respectively. For the spin-polarized state, the number of electrons is $N = 16$ and the parameter $2S$ is 24, while for the spin-unpolarized state $N = 10$ and $2S = 12$.

field, $B \sim 5$ T, the $\nu = \frac{2}{3}$ state in LL-2 should show spin transition into an unpolarized state within a narrow interval of U at the ACP. A strong Zeeman energy >2 meV (for $B = 5$ T) will suppress this spin transition [see Appendix].

In a large magnetic field [Fig. 5(b)], the $\nu = \frac{2}{3}$ state shows interesting spin properties. While in LL-1 the $\nu = \frac{2}{3}$ ground state is spin-unpolarized for small values of U, it becomes spin-polarized for large bias voltage, $U > 420$ meV. In LL-2 the ground state is spin-polarized for all values of U. Finally, combining these two behaviors and comparing the ground state energies of different systems [Fig. 5(b)], we predict the following spin transitions.[22] If the system is initially in LL-1 for the $\nu = \frac{2}{3}$-FQHE state, then with increasing bias voltage the system will undergo the following transitions: **spin-unpolarized** state in LL-1 $\leftrightarrow$ **spin-polarized** state in LL-2 $\Leftrightarrow$ **spin-unpolarized** state in LL-1 $\Leftrightarrow$ **spin-polarized** state in LL-1. What is remarkable here is that spin polarization of the $\nu = \frac{2}{3}$ state in TLG can be controlled by fine tuning the bias voltage, a possibility that never existed in the FQHE regime of conventional systems. The spin transitions for $\nu = \frac{2}{3}$ exist for a small Zeeman energy $\lesssim$1.5 meV [see Appendix].

We have also studied $\nu = \frac{2}{5}$ in LL-1 and LL-2, and find the general properties to be similar to that for $\nu = \frac{1}{3}$, but no spin transitions.[23] In the above analysis we discussed the properties of TLG as a function of the bias voltage and the magnetic field for fixed values of other parameters. Variation of these parameters changes the positions of anticrossing transitions and the values of ACGs, which show most sensitivity to the values of γ_2 and γ_5.

IV. CONCLUDING REMARKS

Trilayer graphene exhibits several very unique electronic properties near the ACPs of two Landau levels. In the FQHE regime the electron-electron interaction strongly renormalizes the ACG. In a weak magnetic field ($B < 8$ T), the many-body interaction enhances the ACG, resulting in a nonmonotonic dependence of the excitation gaps on the bias voltage. In a large magnetic field ($B > 8$ T), the electron-electron interaction strongly suppresses and finally closes the ACG. In that case, the spin-polarized FQHE state shows nontrivial transitions as a function of the bias voltage, which are accompanied by jumps of the FQHE gaps.

In a large magnetic field ($B > 8$ T) the TLG displays unique spin polarizations with *controllable spin transitions*: With the bias voltage the $\nu = \frac{2}{3}$-FQHE state can be switched from spin-polarized to spin-unpolarized states. These spin transitions are due to modification of the interelectron interaction near the ACP, and are different from those in conventional systems.[18,21]

In conventional semiconductor systems the spin transitions are determined by a competition between the Zeeman energy and the difference between cohesive energies of spin-polarized and spin-unpolarized ground states. The origin of spin transitions in conventional systems is therefore the Zeeman energy.

In the TLG system the spin transitions are determined by the modification of interaction potentials in a given Landau level. This modification is due to anticrossing of energy levels, which affects the single particles wave functions and correspondingly changes the interelectron interaction strength. Therefore in the case of TLG, by variation of the parameters of the system, e.g., the bias voltage, we can change the interelectron interaction and even for zero Zeeman energy we can observe spin transitions at the $\nu = \frac{2}{3}$ filling factor. In TLG the spin transition is therefore due to a competition between the cohesive energies of spin-polarized and spin-unpolarized states. Although the TLG system shows many crossings and anticrossings of the Landau levels, only at one special anticrossing point (shown in Fig. 2) can the spin transitions be observed. Therefore, the system needs to be fine tuned to that specific point. Various experimental techniques were developed in the past to study spin transitions in the FQHE regime for conventional electron systems.[18,21] Similar experiments in trilayer graphene will undoubtedly uncover a wealth of information about charge and spin transitions in the FQHE regime.

ACKNOWLEDGMENT

The work has been supported by the Canada Research Chairs Program of the Government of Canada.

APPENDIX: SPIN TRANSITIONS IN TRILAYER GRAPHENE IN THE $\frac{2}{3}$-FQHE FOR A FINITE ZEEMAN ENERGY

The results for the ground state energies of the $\frac{2}{3}$-FQHE systems, shown in Figs. 5(a) and 5(b), correspond to zero Zeeman energy. The finite Zeeman energy, which affects only the spin-polarized states, changes the relative energies of the ground states of spin-polarized and spin-unpolarized phases. The Zeeman energy is defined as $\Delta_z(B) = g_s \mu_B B$ and depends on the magnetic field B and the effective g factor of electrons in trilayer graphene g_s. Here μ_B is the Bohr magneton. For a graphene layer the g factor is around 2. Introducing the Zeeman energy as a parameter, we construct the phase diagram shown in Fig. 6 with two phases corresponding to the spin-polarized and spin-unpolarized ground states. The variables in this diagram are the Zeeman energy Δ_z and the bias voltage U. Here we assume that the g factor of electrons in trilayer graphene is the same as in a single-layer graphene, i.e., $g_s \approx 2$. Then the Zeeman energy is $\Delta_z \approx 0.58$ meV for $B = 5$ T and $\Delta_z \approx 1.7$ meV for $B = 15$ T.

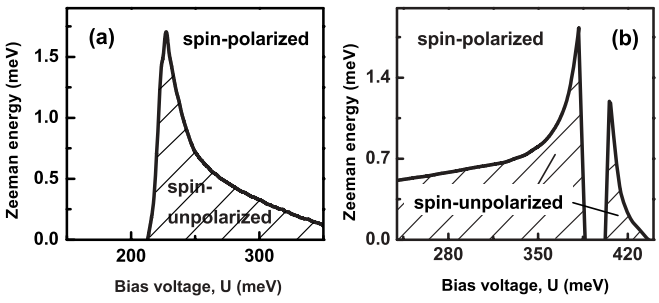

FIG. 6. The phase diagram of the spin-polarized and spin-unpolarized ground state of the system. The phase diagram is shown for the two variables, the Zeeman energy and the bias voltage. The dashed region corresponds to the spin-unpolarized state. The results are shown for $\nu = 2/3$ and magnetic fields $B = 5$ T and $B = 15$ T. The number of electrons in the system is $N = 16$.

*tapash@physics.umanitoba.ca

[1]K. S. Novoselov, Rev. Mod. Phys. **83**, 837 (2011); A. K. Geim, *ibid.* **83**, 851 (2011).

[2]D. S. L. Abergel, V. Apalkov, J. Berashevich, K. Ziegler, and T. Chakraborty, Adv. Phys. **59**, 261 (2010).

[3]K. S. Novoselov, A. K. Geim, S. V. Morozov, D. Jiang, M. I. Katsnelson, I. V. Grigorieva, S. V. Dubonos, and A. A. Firsov, Nature (London) **438**, 197 (2005); Y. Zhang, Y.-W. Tan, H. L. Stormer, and P. Kim, *ibid.* **438**, 201 (2005).

[4]Z. Jiang, E. A. Henriksen, L. C. Tung, Y.-J. Wang, M. E. Schwartz, M. Y. Han, P. Kim, and H. L. Stormer, Phys. Rev. Lett. **98**, 197403 (2007); Y. Zhang, Z. Jiang, J. P. Small, M. S. Purewal, Y.-W. Tan, M. Fazlollahi, J. D. Chudow, J. A. Jaszczak, H. L. Stormer, and P. Kim, *ibid.* **96**, 136806 (2006).

[5]P. R. Wallace, Phys. Rev. **71**, 622 (1947).

[6]K. S. Novoselov, E. McCann, S. V. Morozov, V. I. Fal'Ko, M. I. Katsnelson, U. Zeitler, D. Jiang, F. Schedin, and A. K. Geim, Nat. Phys. **2**, 177 (2006).

[7]J. W. McClure, Phys. Rev. **104**, 666 (1956); R. R. Haering and P. R. Wallace, J. Phys. Chem. Solids **3**, 253 (1957).

[8]E. McCann and V. I. Fal'ko, Phys. Rev. Lett. **96**, 086805 (2006); E. McCann, Phys. Rev. B **74**, 161403(R) (2006); J. M. Pereira Jr., F. M. Peeters, and P. Vasilopoulos, *ibid.* **76**, 115419 (2007).

[9]D. C. Tsui, H. L. Störmer, and A. C. Gossard, Phys. Rev. Lett. **48**, 1559 (1982); R. B. Laughlin, *ibid.* **50**, 1395 (1983).

[10]T. Chakraborty and P. Pietiläinen, *The Quantum Hall Effects* (Springer, New York 1995) 2nd ed.

[11]V. M. Apalkov and T. Chakraborty, Phys. Rev. Lett. **97**, 126801 (2006).

[12]V. M. Apalkov and T. Chakraborty, Phys. Rev. Lett. **105**, 036801 (2010); **107**, 186803 (2011).

[13]X. Du, I. Skachko, F. Duerr, A. Luican, and E. Y. Andrei, Nature (London) **462**, 192 (2009); D. A. Abanin, I. Skachko, X. Du, E. Y. Andrei, and L. S. Levitov, Phys. Rev. B **81**, 115410 (2010); I. Skachko, X. Du, F. Duerr, A. Luican, D. A. Abanin, L. S. Levitov, and E. Y. Andrei, Phil. Trans. R. Soc. A **368**, 5403 (2010).

[14]K. I. Bolotin, F. Ghahari, M. D. Shulman, H. L. Stormer, and P. Kim, Nature (London) **462**, 196 (2009); F. Ghahari, Y. Zhao, P. Cadden-Zimansky, K. Bolotin, and P. Kim, Phys. Rev. Lett. **106**, 046801 (2011).

[15]M. Koshino and E. McCann, Phys. Rev. B **83**, 165443 (2011); S. Yuan, R. Roldan, and M. I. Katsnelson, *ibid.* **84**, 125455 (2011); S. H. R. Sena, J. M. Pereira Jr., F. M. Peeters, and G. A. Farias, *ibid.* **84**, 205448 (2011).

[16]T. Taychatanapat, K. Watanabe, T. Taniguchi, and P. Jarillo-Herrero, Nat. Phys. **7**, 621 (2011); A. Kumar, W. Escoffier, J. M. Poumirol, C. Faugeras, D. P. Arovas, M. M. Fogler, F. Guinea, S. Roche, M. Goiran, and B. Raquet, Phys. Rev. Lett. **107**, 126806 (2011).

[17]T. Chakraborty, Adv. Phys. **49**, 959 (2000); T. Chakraborty, P. Pietiläinen, and F. C. Zhang, Phys. Rev. Lett. **57**, 130 (1986); T. Chakraborty, Surf. Sci. **229**, 16 (1990); T. Chakraborty and F. C. Zhang, Phys. Rev. B **29**, 7032 (1984); F. C. Zhang and T. Chakraborty, *ibid.* **34**, 7076 (1986); T. Chakraborty and P. Pietiläinen, *ibid.* **39**, 7971 (1989); **41**, 10862 (1990); Phys. Rev. Lett. **76**, 4018 (1996); **83**, 5559 (1999).

[18]R. G. Clark, S. R. Haynes, A. M. Suckling, J. R. Mallett, P. A. Wright, J. J. Harrish, and C. T. Foxon, Phys. Rev. Lett. **62**, 1536 (1989); J. P. Eisenstein, H. L. Störmer, L. Pfeiffer, and K. W. West, *ibid.* **62**, 1540 (1989); A. G. Davis, R. Newbury, M. Pepper, J. E. F. Frost, D. A. Ritchie, and G. A. C. Jones, Phys. Rev. B **44**, 13128 (1991); L. W. Engel, S. W. Hwang, T. Sajoto, D. C. Tsui, and M. Shayegan, *ibid.* **45**, 3418 (1992); T. Sajoto, Y. W. Suen, L. W. Engel, M. B. Santos, and M. Shayegan, *ibid.* **41**, 8449 (1990).

[19]F. D. M. Haldane, Phys. Rev. Lett. **51**, 605 (1983).

[20]If the TLG is in an incompressible state with a finite FQHE gap, then the numerical results are stable and show weak dependence on the number of particles, N. For a compressible state with almost zero FQHE gap, the energy of the ground state of the system depends on N but this dependence does not affect our conclusions, which are based on the behavior of incompressible states.

[21]W. Kang, J. B. Young, S. T. Hannahs, E. Palm, K. L. Chapman, and A. C. Gossard, Phys. Rev. B **56**, 12776(R) (1997); H. Cho, J. B. Young, W. Kang, K. L. Chapman, M. Bichler, and W. Wegscheider, Phys. Rev. Lett. **81**, 2522 (1998); P. Khandelwal, N. N. Kuzma, S. E. Berrett, L. N. Pfeiffer, and K. W. West, *ibid.* **81**, 673 (1998); L. A. Tracy, J. P. Eisenstein, L. N. Pfeiffer, and K. W. West, *ibid.* **98**, 086801 (2007); O. Stern, D. Dini, N. Freytag, W. Dietsche, K. von Klitzing, and W. Wegscheider, Phys. Status Solidi B **245**, 428 (2008); I. V. Kukushkin, K. von Klitzing, and K. Eberl, Phys. Rev. B **55**, 10607 (1997).

[22]When comparing the energies of different states, we consider that if the difference between the ground state energies of spin-polarized and spin-unpolarized states is small (e.g., <0.5 meV), then even for a small Zeeman energy the TLG is spin-polarized.

[23]At the ACP, the $\nu = \frac{2}{5}$ state shows an enhancement of the ACG for a small magnetic field and strong suppression of the ACG for large magnetic fields. For both LL-1 and LL-2, the ground state is spin polarized and excludes the possibility of any spin transition.